

1.4 Magnetic interactions

In the metallic state, the $4f$ electrons on a rare earth ion are subjected to a variety of interactions with their surroundings. These forces may be broadly classified into two categories. The *single-ion interactions* act independently at each ionic site, so that their influence on the state of the $4f$ electrons at a particular site is unaffected by the magnetic state of its neighbours. The corresponding contribution to the Hamiltonian therefore contains sums over terms located at the ionic sites i of the crystal, but without any coupling between different ions. On the other hand, the *two-ion interactions* couple the $4f$ -electron clouds at pairs of ions, giving terms which involve two sites i and j .

The charge distribution around an ion produces an electric field, with the local point-symmetry, which acts on the $4f$ electrons and gives rise to the large magnetic anisotropies which are characteristic of the rare earth metals. This *crystal field* makes a contribution to the potential energy of a $4f$ electron with charge $-e$

$$v_{\text{cf}}(\mathbf{r}) = - \int \frac{e\rho(\mathbf{R})}{|\mathbf{r} - \mathbf{R}|} d\mathbf{R}, \quad (1.4.1)$$

where $\rho(\mathbf{R})$ is the charge density of the surrounding electrons and nuclei. If these do not penetrate the $4f$ charge cloud, $v_{\text{cf}}(\mathbf{r})$ is a solution of Laplace's equation, and may be expanded in spherical harmonics as

$$v_{\text{cf}}(\mathbf{r}) = \sum_{lm} A_l^m r^l Y_{lm}(\hat{\mathbf{r}}), \quad (1.4.2)$$

where

$$A_l^m = -(-1)^m \frac{4\pi}{2l+1} \int \frac{e\rho(\mathbf{R})}{R^{l+1}} Y_{l-m}(\hat{\mathbf{R}}) d\mathbf{R}, \quad (1.4.3)$$

which is a special case of the multipole expansion (1.3.7). We can thus look upon (1.4.2) as arising from the interaction of the multipoles $r^l Y_{lm}(\hat{\mathbf{r}})$ of the $4f$ electrons with the appropriate components of the electric field. If part of the charge which is responsible for the crystal field lies within the $4f$ cloud, $v_{\text{cf}}(\mathbf{r})$ can still be expanded in spherical

harmonics with the appropriate symmetry, but the coefficients are not generally proportional to r^l , nor to (1.4.3).

As the crystal-field energy is small compared to the spin-orbit splitting, its effects on the eigenstates of the system are adequately accounted for by first-order perturbation theory. Since f electrons cannot have multipole distributions with $l > 6$, the properties of the spherical harmonics ensure that the corresponding matrix elements of (1.4.2) vanish. Even so, the calculation of those that remain from the electronic wavefunctions would be a formidable task, even if the surrounding charge distribution were known, if the ubiquitous Wigner-Eckart theorem did not once again come to the rescue. As first pointed out by Stevens (1952), provided that we remain within a manifold of constant J , in this case the ground-state multiplet, the matrix elements of $v_{\text{cf}}(\mathbf{r})$ are proportional to those of operator equivalents, written in terms of the \mathbf{J} operators. We may thus replace (1.4.2) by

$$\mathcal{H}_{\text{cf}} = \sum_i \sum_{lm} A_l^m \alpha_l \langle r^l \rangle \left(\frac{2l+1}{4\pi} \right)^{1/2} \tilde{O}_{lm}(\mathbf{J}_i), \quad (1.4.4)$$

where we have also summed over the ions. The *Stevens factors* α_l depend on the form of the electronic charge cloud through L , S and J , and on l , but not on m . They are frequently denoted α , β , and γ when l is 2, 4, and 6 respectively, and their values for the magnetic rare earth ions are given in Table 1.4. The expectation value $\langle r^l \rangle$ is an average over the $4f$ states. The *Racah operators* $\tilde{O}_{lm}(\mathbf{J})$ are obtained from the spherical harmonics, multiplied by $(4\pi/2l+1)^{1/2}$, by writing them in terms of

Table 1.4. Stevens factors for rare earth ions.

Ion ⁺⁺⁺	$\alpha \times 10^2$	$\beta \times 10^4$	$\gamma \times 10^6$
Ce	-5.714	63.49	0
Pr	-2.101	-7.346	60.99
Nd	-0.6428	-2.911	-37.99
Pm	0.7714	4.076	60.78
Sm	4.127	25.01	0
Tb	-1.0101	1.224	-1.121
Dy	-0.6349	-0.5920	1.035
Ho	-0.2222	-0.3330	-1.294
Er	0.2540	0.4440	2.070
Tm	1.0101	1.632	-5.606
Yb	3.175	-17.32	148.0

Cartesian coordinates and replacing (x, y, z) by (J_x, J_y, J_z) , with an appropriate symmetrization to take account of the non-commutation of the \mathbf{J} operators. They have been tabulated for l -values up to 8 by Lindgård and Danielsen (1974).

Following the customary practice, we shall generally use not the Racah operators, which are tensor operators transforming under rotations like spherical harmonics, but the *Stevens operators* $O_l^m(\mathbf{J})$, which transform like the real *tesseral harmonics* T_{lm} . If we define corresponding operators for m zero or positive as:

$$\begin{aligned} T_{l0} &= \tilde{O}_{l0} \\ T_{lm}^c &= \frac{1}{\sqrt{2}} [\tilde{O}_{l-m} + (-1)^m \tilde{O}_{lm}] \\ T_{lm}^s &= \frac{i}{\sqrt{2}} [\tilde{O}_{l-m} - (-1)^m \tilde{O}_{lm}], \end{aligned} \quad (1.4.5)$$

the Stevens operators for positive and negative m are proportional respectively to T_{lm}^c and $T_{l|m|}^s$. There is some ambiguity in the literature about the proportionality constants, but we have used the standard definitions of the Stevens operators in Table 1.5, see also Hutchings (1964). In terms of these operators, we may write the crystal-field Hamiltonian

$$\mathcal{H}_{\text{cf}} = \sum_i \sum_{lm} B_l^m O_l^m(\mathbf{J}_i). \quad (1.4.6a)$$

The *crystal-field parameters* B_l^m can in principle be calculated from the charge distribution in the metal, but in practice attempts to do so have met with limited success. The difficulties are two-fold. The charge density on the surroundings of an ion is not easy to determine with the necessary accuracy, and the approximations normally used in the calculation of the electronic structure of a metal, in particular the assumption that the charge distribution in the atomic polyhedron is spherically symmetric, are inadequate for the purpose. Furthermore, a redistribution of the charge within the cell can modify the electric fields experienced by the $4f$ electrons, and such shielding effects are again very difficult to estimate. It is therefore necessary to appeal to relatively crude models, such as the instructive but quite unjustified point-charge model, in which an adjustable charge is placed on each lattice site, or alternatively to regard the B_l^m as parameters to be determined from experiment.

Fortunately, the number of such parameters is strongly restricted by symmetry. We shall be concerned almost exclusively with the hexagonal structures of Fig. 1.3, and in defining the Stevens operators, we have used a Cartesian system in which the (x, y, z) -directions are along the

Table 1.5. Stevens operators. $X \equiv J(J+1)$ and $J_{\pm} \equiv J_x \pm iJ_y$.

O_2^2	$= \frac{1}{2}(J_+^2 + J_-^2)$
O_2^1	$= \frac{1}{2}(J_z J_x + J_x J_z)$
O_2^0	$= 3J_z^2 - X$
O_2^{-1}	$= \frac{1}{2}(J_z J_y + J_y J_z)$
O_2^{-2}	$= \frac{1}{2i}(J_+^2 - J_-^2)$
O_4^4	$= \frac{1}{2}(J_+^4 + J_-^4)$
O_4^2	$= \frac{1}{4}[(7J_z^2 - X - 5)(J_+^2 + J_-^2) + (J_+^2 + J_-^2)(7J_z^2 - X - 5)]$
O_4^0	$= 35J_z^4 - (30X - 25)J_z^2 + 3X^2 - 6X$
O_4^{-2}	$= \frac{1}{4i}[(7J_z^2 - X - 5)(J_+^2 - J_-^2) + (J_+^2 - J_-^2)(7J_z^2 - X - 5)]$
O_4^{-4}	$= \frac{1}{2i}(J_+^4 - J_-^4)$
O_6^0	$= 231J_z^6 - (315X - 735)J_z^4 + (105X^2 - 525X + 294)J_z^2$ $\quad\quad\quad - 5X^3 + 40X^2 - 60X$
O_6^6	$= \frac{1}{2}(J_+^6 + J_-^6)$

crystallographic (a, b, c) -axes specified in the previous section. However, it will later be convenient to rotate the z -axis into the magnetization direction, and instead orient the crystallographic (a, b, c) -axes along the (ξ, η, ζ) -Cartesian directions. For an ion with hexagonal point-symmetry, as in the hcp structure or on the hexagonal sites of the dhcp structure, the crystal field is specified by 4 parameters:

$$\mathcal{H}_{\text{cf}} = \sum_i \left[\sum_{l=2,4,6} B_l^0 O_l^0(\mathbf{J}_i) + B_6^6 O_6^6(\mathbf{J}_i) \right]. \quad (1.4.6b)$$

The Hamiltonian (1.4.6) lifts the degeneracy of the ionic $|JM_J\rangle$ states and, since it is expressed in terms of \mathbf{J} operators, whose matrix elements between these states may be determined by straightforward calculation, it may readily be diagonalized to yield the crystal-field energies and eigenfunctions. The B_l^m may then be used as adjustable parameters to reproduce the available experimental information on these eigenstates. As an example, we show in Fig. 1.16 the splitting of the nine $|4M_J\rangle$ states in Pr by the crystal fields acting on the hexagonal sites. This level scheme was derived from values of the crystal-field parameters adjusted

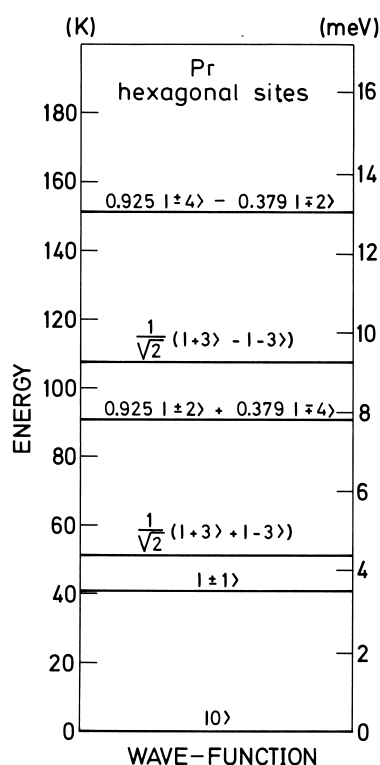


Fig. 1.16. The crystal-field splitting of the nine $|4M_J\rangle$ states on the hexagonal sites in dhcp Pr. The wavefunctions are written in terms of a basis $|M_J\rangle$ corresponding to quantization along the c -direction.

to account for a variety of experimental phenomena (Houmann *et al.* 1979).

If the lattice is strained, the crystal fields, and indeed all the other magnetic interactions which we shall discuss, are modified. In consequence, there is a *magnetoelastic coupling* between the moments and the strain, which can have profound consequences for rare earth magnetism. Magnetoelastic effects are manifested in both single-ion and two-ion terms in the Hamiltonian, though we shall mostly be concerned with the former. The elastic energy is quadratic in the strain, measured relative to the equilibrium configuration in the absence of magnetic interactions. The magnetoelastic energy is linear in the strain and the competition between the two effects may lead to some equilibrium strain or *magnetostriction*. Because of their moderate elastic constants and the large orbital component in their moments, the lanthanide metals display the largest known magnetostrictions.

Following Callen and Callen (1965), it is convenient to develop the theory in terms of the irreducible strains for hexagonal point-symmetry,

which are related to the Cartesian strains as follows:

$$\begin{aligned}
\epsilon_{\alpha 1} &= \epsilon_{11} + \epsilon_{22} + \epsilon_{33} \\
\epsilon_{\alpha 2} &= \frac{1}{3}(2\epsilon_{33} - \epsilon_{11} - \epsilon_{22}) \\
\epsilon_{\gamma 1} &= \frac{1}{2}(\epsilon_{11} - \epsilon_{22}) \\
\epsilon_{\gamma 2} &= \epsilon_{12} \\
\epsilon_{\varepsilon 1} &= \epsilon_{13} \\
\epsilon_{\varepsilon 2} &= \epsilon_{23},
\end{aligned} \tag{1.4.7}$$

where we have adopted the conventional notation of designating the Cartesian axes (ξ, η, ζ) by $(1, 2, 3)$. The α -strains are thus symmetry-conserving dilatations, the γ -strains distort the hexagonal symmetry of the basal plane, and the ε -strains shear the c -axis. The elastic energy may then be written

$$\begin{aligned}
\mathcal{H}_{\text{el}} = N \left[\frac{1}{2}c_{\alpha 1}\epsilon_{\alpha 1}^2 + c_{\alpha 3}\epsilon_{\alpha 1}\epsilon_{\alpha 2} + \frac{1}{2}c_{\alpha 2}\epsilon_{\alpha 2}^2 \right. \\
\left. + \frac{1}{2}c_{\gamma}(\epsilon_{\gamma 1}^2 + \epsilon_{\gamma 2}^2) + \frac{1}{2}c_{\varepsilon}(\epsilon_{\varepsilon 1}^2 + \epsilon_{\varepsilon 2}^2) \right],
\end{aligned} \tag{1.4.8}$$

where we have defined irreducible elastic stiffness constants per ion, related to the five independent Cartesian constants by

$$\begin{aligned}
c_{\alpha 1} &= \frac{1}{9}(2c_{11} + 2c_{12} + 4c_{13} + c_{33})V/N \\
c_{\alpha 2} &= \frac{1}{2}(c_{11} + c_{12} - 4c_{13} + 2c_{33})V/N \\
c_{\alpha 3} &= \frac{1}{3}(-c_{11} - c_{12} + c_{13} + c_{33})V/N \\
c_{\gamma} &= 2(c_{11} - c_{12})V/N \\
c_{\varepsilon} &= 4c_{44}V/N.
\end{aligned} \tag{1.4.9}$$

The contributions to the single-ion magnetoelastic Hamiltonian, corresponding to the different irreducible strains, are

$$\begin{aligned}
\mathcal{H}_{\text{me}}^{\alpha} = - \sum_i \left[\sum_{l=2,4,6} \{B_{\alpha 1}^l \epsilon_{\alpha 1} + B_{\alpha 2}^l \epsilon_{\alpha 2}\} O_l^0(\mathbf{J}_i) \right. \\
\left. + \{B_{\alpha 1}^{66} \epsilon_{\alpha 1} + B_{\alpha 2}^{66} \epsilon_{\alpha 2}\} O_6^6(\mathbf{J}_i) \right]
\end{aligned} \tag{1.4.10}$$

$$\begin{aligned}
\mathcal{H}_{\text{me}}^{\gamma} = - \sum_i \left[\sum_{l=2,4,6} B_{\gamma 2}^l \{O_l^2(\mathbf{J}_i) \epsilon_{\gamma 1} + O_l^{-2}(\mathbf{J}_i) \epsilon_{\gamma 2}\} \right. \\
\left. + \sum_{l=4,6} B_{\gamma 4}^l \{O_l^4(\mathbf{J}_i) \epsilon_{\gamma 1} - O_l^{-4}(\mathbf{J}_i) \epsilon_{\gamma 2}\} \right]
\end{aligned} \tag{1.4.11}$$

$$\begin{aligned}
\mathcal{H}_{\text{me}}^{\varepsilon} = - \sum_i \left[\sum_{l=2,4,6} B_{\varepsilon 1}^l \{O_l^1(\mathbf{J}_i) \epsilon_{\varepsilon 1} + O_l^{-1}(\mathbf{J}_i) \epsilon_{\varepsilon 2}\} \right. \\
\left. + B_{\varepsilon 5} \{O_6^5(\mathbf{J}_i) \epsilon_{\varepsilon 1} - O_6^{-5}(\mathbf{J}_i) \epsilon_{\varepsilon 2}\} \right].
\end{aligned} \tag{1.4.12}$$

The operators in the α -strain term are the same as those in the crystal-field Hamiltonian (1.4.6b), and the associated magnetoelastic effects may thus be considered as a strain-dependent renormalization of the crystal-field parameters, except that these interactions may mediate a dynamical coupling between the magnetic excitations and the phonons. The other two terms may have the same effect, but they also modify the symmetry and, as we shall see, can therefore qualitatively influence both the magnetic structures and excitations.

It is the two-ion couplings which are primarily responsible for cooperative effects and magnetic ordering in the rare earths, and of these the most important is the *indirect exchange*, by which the moments on pairs of ions are coupled through the intermediary of the conduction electrons. The form of this coupling can be calculated straightforwardly, provided that we generalize (1.3.22) slightly to

$$\mathcal{H}_{\text{sf}}(i) = -2 \int I(\mathbf{r} - \mathbf{R}_i) \mathbf{S}_i \cdot \mathbf{s}(\mathbf{r}) d\mathbf{r} = - \int \mathbf{H}_i(\mathbf{r}) \cdot \boldsymbol{\mu}(\mathbf{r}) d\mathbf{r}, \quad (1.4.13)$$

$\mathbf{s}(\mathbf{r})$ is the conduction-electron spin density, and the exchange integral $I(\mathbf{r} - \mathbf{R}_i)$ is determined by the overlap of the $4f$ and conduction-electron charge clouds. This expression, whose justification and limitations will be discussed in Section 5.7, can be viewed as arising from the action of the effective inhomogeneous magnetic field

$$\mathbf{H}_i(\mathbf{r}) = \frac{1}{\mu_B} I(\mathbf{r} - \mathbf{R}_i) \mathbf{S}_i = \frac{1}{\mu_B N} \sum_{\mathbf{q}} I(\mathbf{q}) e^{i\mathbf{q} \cdot (\mathbf{r} - \mathbf{R}_i)} \mathbf{S}_i \quad (1.4.14)$$

on the conduction-electron moment density $\boldsymbol{\mu}(\mathbf{r}) = 2\mu_B \mathbf{s}(\mathbf{r})$. The spin at \mathbf{R}_i generates a moment at \mathbf{r} , whose Cartesian components are given by

$$\mu_{i\alpha}(\mathbf{r}) = \frac{1}{V} \sum_{\beta} \int \chi_{\alpha\beta}(\mathbf{r} - \mathbf{r}') H_{i\beta}(\mathbf{r}') d\mathbf{r}', \quad (1.4.15)$$

where $\bar{\chi}$ is the nonlocal susceptibility tensor for the conduction electrons and V the volume. This induced moment interacts through $\mathcal{H}_{\text{sf}}(j)$ with the spin \mathbf{S}_j , leading to a coupling

$$\mathcal{H}(ij) = -\frac{1}{V} \sum_{\alpha\beta} \iint H_{j\alpha}(\mathbf{r}) \chi_{\alpha\beta}(\mathbf{r} - \mathbf{r}') H_{i\beta}(\mathbf{r}') d\mathbf{r} d\mathbf{r}'. \quad (1.4.16)$$

If we neglect, for the moment, the spin-orbit coupling of the conduction electrons, and the crystal is unmagnetized, $\chi_{\alpha\beta}$ becomes a scalar. The Fourier transform is:

$$\chi(\mathbf{q}) = \frac{1}{V} \int \chi(\mathbf{r}) e^{-i\mathbf{q} \cdot \mathbf{r}} d\mathbf{r} \quad (1.4.17)$$

in terms of which the integrations with respect to \mathbf{r} and \mathbf{r}' in eqn (1.4.16) are calculated straightforwardly. Summing the result over the N lattice sites, counting each interaction once only, we find that the indirect-exchange interaction takes the familiar isotropic Heisenberg form:

$$\begin{aligned}\mathcal{H}_{\text{ff}} &= -\frac{1}{2} \frac{V}{N^2 \mu_B^2} \sum_{ij} \sum_{\mathbf{q}} \chi(\mathbf{q}) I(\mathbf{q}) I(-\mathbf{q}) e^{i\mathbf{q} \cdot (\mathbf{R}_i - \mathbf{R}_j)} \mathbf{S}_i \cdot \mathbf{S}_j \\ &= -\frac{1}{2N} \sum_{\mathbf{q}} \sum_{ij} \mathcal{J}_S(\mathbf{q}) e^{i\mathbf{q} \cdot (\mathbf{R}_i - \mathbf{R}_j)} \mathbf{S}_i \cdot \mathbf{S}_j \\ &= -\frac{1}{2} \sum_{ij} \mathcal{J}_S(ij) \mathbf{S}_i \cdot \mathbf{S}_j,\end{aligned}\tag{1.4.18}$$

where

$$\mathcal{J}_S(ij) = \frac{1}{N} \sum_{\mathbf{q}} \mathcal{J}_S(\mathbf{q}) e^{i\mathbf{q} \cdot (\mathbf{R}_i - \mathbf{R}_j)}\tag{1.4.19}$$

and

$$\mathcal{J}_S(\mathbf{q}) = \sum_j \mathcal{J}_S(ij) e^{-i\mathbf{q} \cdot (\mathbf{R}_i - \mathbf{R}_j)} = \frac{V}{N \mu_B^2} |I(\mathbf{q})|^2 \chi(\mathbf{q}).\tag{1.4.20}$$

In the presence of an orbital moment, it is convenient to express (1.4.18) in terms of \mathbf{J} rather than \mathbf{S} , which we may do within the ground-state multiplet by using (1.2.29) to project \mathbf{S} on to \mathbf{J} , obtaining

$$\mathcal{H}_{\text{ff}} = -\frac{1}{2} \sum_{ij} \mathcal{J}(ij) \mathbf{J}_i \cdot \mathbf{J}_j,\tag{1.4.21}$$

with

$$\mathcal{J}(\mathbf{q}) = (g-1)^2 \left[\mathcal{J}_S(\mathbf{q}) - \frac{1}{N} \sum_{\mathbf{q}'} \mathcal{J}_S(\mathbf{q}') \right],\tag{1.4.22}$$

where we have also subtracted the interaction of the i th moment with itself, as this term only leads to the constant contribution to the Hamiltonian; $-\frac{1}{2}(g-1)^2 N \mathcal{J}_S(ii) J(J+1)$. The origin of the indirect exchange in the polarization of the conduction-electron gas by the spin on one ion, and the influence of this polarization on the spin of a second ion, is apparent in the expression (1.4.20) for $\mathcal{J}_S(\mathbf{q})$. As we shall see, it is the Fourier transform $[\mathcal{J}(\mathbf{q}) - \mathcal{J}(\mathbf{0})]$ which may be directly deduced from measurements of the dispersion relations for the magnetic excitations, and its experimentally determined variation with \mathbf{q} in the c -direction for the heavy rare earths is shown in Fig. 1.17.

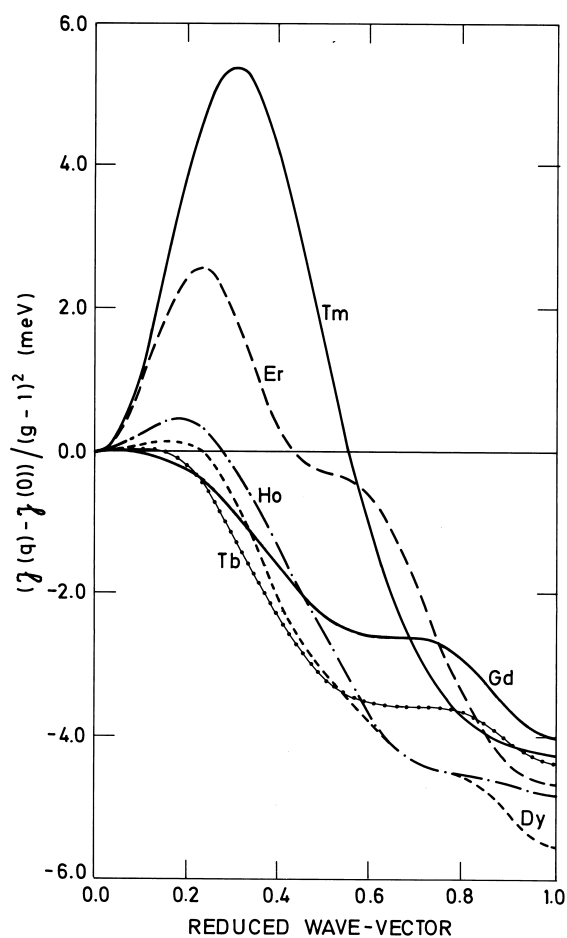


Fig. 1.17. The exchange interaction $\mathcal{J}_S(\mathbf{q}) - \mathcal{J}_S(\mathbf{0})$, determined experimentally in the magnetic heavy rare earth metals. The magnitude of the peak, which stabilizes the observed periodic magnetic structures, increases monotonically with atomic number.

A notable feature is the maximum which, except in Gd, occurs at non-zero \mathbf{q} and, as discussed in the following section, is responsible for stabilizing the periodic magnetic structures in the metals. In the approximation which we have used, the conduction-electron susceptibility is given by

$$\chi(\mathbf{q}) = \frac{2\mu_B^2}{V} \sum_{nn'\mathbf{k}} \frac{f_{n\mathbf{k}} - f_{n'\mathbf{k}-\mathbf{q}}}{\varepsilon_{n'}(\mathbf{k}-\mathbf{q}) - \varepsilon_n(\mathbf{k})}, \quad (1.4.23)$$

where $f_{n\mathbf{k}}$ is the Fermi–Dirac function. It is clear that a large contribution to the sum is made by pairs of electronic states, separated by \mathbf{q} , one of which is occupied and the other empty, and both of which have energies very close to the Fermi level. Consequently, parallel or *nesting* regions of the Fermi surface tend to produce peaks, known as *Kohn anomalies*, at the wave-vector \mathbf{Q} which separates them, and it is believed that the parallel sections of the webbing in the hole surface of Fig. 1.11 give rise to the maxima shown in Fig. 1.17. As we have mentioned, this conjecture is supported by both positron-annihilation experiments and band structure calculations but, despite extensive efforts, first-principles estimates of $\mathcal{J}(\mathbf{q})$ have not proved particularly successful. $\chi(\mathbf{q})$ may be calculated quite readily from the energy bands (Liu 1978), and exhibits the expected peaks, but the exchange matrix elements which determine $I(\mathbf{q})$ are much less tractable. Lindgård *et al.* (1975) obtained the correct general variation with \mathbf{q} for Gd, but the matrix elements were, not surprisingly, far too large when the screening of the Coulomb interaction was neglected.

The Kohn anomalies in $\mathcal{J}(\mathbf{q})$ Fourier transform into *Friedel oscillations* in $\mathcal{J}(\mathbf{R})$, and such oscillations, and the extremely long range of the indirect exchange, are illustrated in the results of Houmann *et al.* (1979) for Pr in Fig. 1.18. As is also shown in this figure, they found that the *anisotropic* component of the coupling is a substantial proportion of the Heisenberg exchange. The anisotropic coupling between the moments on two ions can be written in the general form

$$\mathcal{H}_{JJ} = -\frac{1}{2} \sum_{ij} \sum_{l'l'mm'} \mathcal{K}_{ll'mm'}^{m'm'}(ij) O_l^m(\mathbf{J}_i) O_{l'}^{m'}(\mathbf{J}_j), \quad (1.4.24)$$

where the terms which appear in the sum are restricted by symmetry, but otherwise may exhibit a large variety, depending on their origin. The many possible causes of anisotropy have been summarized by Jensen *et al.* (1975). They are usually associated with the orbital component of the moment and are therefore expected to be relatively large when L is large. In addition to contributions due to the influence of the localized $4f$ orbital moment on the conduction electrons (Kaplan and Lyons 1963), and to the magnetization and spin–orbit coupling of the latter (Levy 1969), direct multipolar interactions and two-ion magnetoelastic couplings, for which the coefficients $\mathcal{K}_{ll'mm'}^{m'm'}$ depend explicitly on the strain, may be important. A general two-ion coupling which depends only on the dipolar moments of the $4f$ electrons is

$$\mathcal{H}_{dd} = -\frac{1}{2} \sum_{ij} \mathcal{J}_{\alpha\beta}(ij) J_{i\alpha} J_{j\beta}. \quad (1.4.25)$$

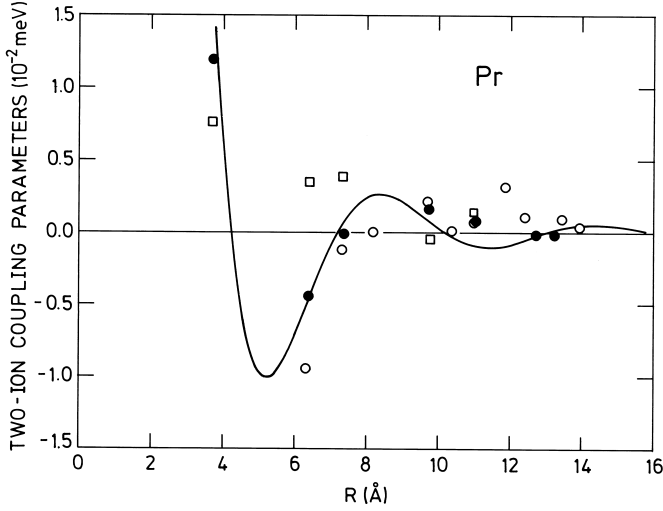


Fig. 1.18. The indirect-exchange interaction between ions on the hexagonal sites in Pr, deduced from measurements of the magnetic excitations at 6 K. The circles represent the isotropic interaction $\mathcal{J}(\mathbf{R})$ between an ion at the origin and those at different sites. The filled symbols are for pairs of ions in the same hexagonal plane, and the open symbols for pairs in different planes. The former are reasonably well described by the simple free-electron model of Section 5.7.1, with an effective value of 1.1 \AA^{-1} for $2k_F$, as shown by the full curve. In addition, the exchange incorporates an anisotropic component $\mathcal{K}(\mathbf{R})$, discussed in Section 2.1.6, which is smaller, but of comparable magnitude. Its values between pairs of ions in the plane are indicated by the squares. The calculated uncertainties in the exchange interactions are, at the most, the size of the points.

The dispersion relations for the magnetic excitations provide extensive evidence for anisotropy of this form. A special case is the classical *dipole-dipole interaction* for which

$$\mathcal{J}_{\alpha\beta}(ij) = (g\mu_B)^2 \frac{3(R_{i\alpha} - R_{j\alpha})(R_{i\beta} - R_{j\beta}) - \delta_{\alpha\beta}|\mathbf{R}_i - \mathbf{R}_j|^2}{|\mathbf{R}_i - \mathbf{R}_j|^5}. \quad (1.4.26)$$

Although it is very weak, being typically one or two orders of magnitude less than the exchange between nearest neighbours, the dipole-dipole coupling is both highly anisotropic and extremely long-ranged, and may therefore have important effects on both magnetic structures and excitations. Apart from this example, the anisotropic two-ion couplings are even more difficult to calculate than are the isotropic components, so the strategy which has generally been adopted to investigate them is to

assume that all terms in (1.4.24) which are not forbidden by symmetry are present, to calculate their influence on the magnetic properties, and to determine their magnitude by judicious experiments.

The *hyperfine interaction* between the $4f$ moment and the nuclear spin \mathbf{I} may be written

$$\mathcal{H}_{\text{hf}} = A \sum_i \mathbf{I}_i \cdot \mathbf{J}_i. \quad (1.4.27)$$

Since A is typically of the order of micro-electron-volts, the coupling to the nuclei normally has a negligible effect on the electronic magnetism in the rare earth metals, but we shall see in Sections 7.3 and 7.4 that it has a decisive influence on the low-temperature ordering in Pr.